

Density Functional Theory and Vibrational spectroscopic studies of 8-hydroxy-5-nitroquinoline

Neredimelli Udaya Sri,* Mandru V S Prasad

Department of Physics, D.N.R. College, Bhimavaram-534 202, A.P., India.

Abstract: A combined experimental and theoretical DFT study of the structural, vibrational and electronic properties of 8-hydroxy-5-nitroquinoline (8H5NQ) is presented using B3LYP function with 6-31G(d, p) basis set. The theoretical geometry optimization data were compared with the X-ray data for a similar structure in the associated literature, showing similar values. In addition, natural bond orbitals (NBOs), HOMO-LUMO energy gap, mapped molecular Electrostatic Potential (MEP) surface calculation, first and second order hyperpolarizabilities were also performed with the same calculation level. Theoretical UV spectrum agreed well with the measured experimental data, with transitions assigned. The molecular electrostatic potential map shows opposite potentials regions that form hydrogen bonds that stabilize the dimeric form, which were confirmed by the close values related to the C=O bond stretching between the dimeric form and the experimental IR spectra. Calculated HOMO-LUMO gaps show the excitation energy for 8H5NQ, justifying its stability and kinetics reaction.

Keywords: DFT, IR and Raman Spectra, HOMO-LUMO, NBO.

I. Introduction

Quinoline is a heterocyclic scaffold of paramount importance to human race. The quinoline ring system occurs in various natural products, especially in alkaloids. Indeed quinoline derivatives are some of the oldest compounds which have been utilized for the treatment of a variety of diseases. In 1820, *quinine* is isolated as the active ingredient from the bark of Cinchona trees and consecutively replaced the crude bark for the treatment of malaria. The bark of Cinchona plant containing quinine is also utilized to treat palpitations [1], fevers and tertian's since more than 200 years ago. Quinoline is first extracted from *coal tar* in 1834 by Friedlieb Ferdinand Runge [2]. Compounds containing quinoline motif are most widely used as antimalarials [3], antibacterials [4], antifungals [5], anticancer agents [6] and HIV-1 Integrase Inhibitor [7].

Additionally, quinoline derivatives find use in the synthesis of fungicides, virucides, biocides, alkaloids, rubber chemicals and flavoring agents [8]. Nitroquinoline, or 8-hydroxy-5-nitroquinoline, shows antibacterial and fungicidal activity. The aminoquinolines are of considerable importance as intermediates in the preparation of dyes and drugs. The precursor of 8-hydroxyquinoline is a versatile chelating agent and precursor to pesticides and 2- and 4-methyl derivatives of quinoline are precursors to cyanine dyes. The molecular formula of parent compound i.e., quinoline is C₆H₇N, the density at 25°C is 1.090, the melting and boiling points at atmospheric pressure are -15°C and 237.64°C respectively. It has strong absorption of light wavelengths greater than 290 nm. Recently, quinoline conjugated derivatives have generated considerable interest as blue-emitting materials [9]. The π -conjugated polyquinolines and related polyquinoxalines have demonstrated excellent electron-transport and electroluminescent properties in OLEDs [10]. Polyquinolines are emerging as very promising blue emitting materials due to their unique combination of high thermal stability, easy processability and high photoluminescence (PL) quantum yields [11].

Literature survey reveals that so far there is no complete experimental and theoretical study for the title compound. In the present study, both experimental and molecular modeling methods are combined for studying the optimized molecular structural parameters, vibrational spectra, thermodynamical parameters, total dipole moment, first hyperpolarizability and HOMO-LUMO energies for 8-hydroxy-5-nitroquinoline (8H5NQ) using DFT/B3LYP method using 6-31G(d,p) basis set.

II. Results and Discussion

Geometrical structure

The first task in the computational work is to determine the optimized geometry of 8H5NQ. The optimized structure parameters calculated with DFT/(B3LYP) method and 6-31G(d,p) basis set are listed in Table 1 in accordance with the atom numbering scheme given in Fig 1. The molecule belongs to the C_s point group with 20 atoms. Our calculated results show that the aromatic ring in 8H5NQ is distorted from regular hexagon due to steric and electronic effects of the electron donating and electron withdrawing substituents. The

crystal data of a closely related molecule [12] is compared with that of 8H5NC. As seen from Table 1 most of the optimized bond lengths are slightly longer than the experimental values and the bond angles are slightly different from the experimental ones, because the molecular states are different during experimental and theoretical processes. One isolated molecule is considered in gas phase in theoretical calculation, whereas many packed molecules are treated in condensed phase during the experimental measurement. However, the theoretical results obtained are almost comparable with the reported structural parameters of the parent molecule. The reported values of C-N bond lengths of different quinoline complexes are 1.307– 1.362 Å [13] and 1.359-1.456 Å [14]. In the present study, the C-N bond length is calculated to be 1.298-1.367Å, which is shorter than the normal C–N single bond length of about 1.48 Å. The shortening of these C–N bonds reveals the effect of resonance in this part of the molecule.



Fig. 1 Molecular structures of 8-hydroxy-5-nitroquinoline obtained along with numbering of atoms.

Table 1: Optimized geometrical parameters of 8-hydroxy-5-nitroquinoline obtained by B3LYP/6-31G(d,p) density functional calculations.

Bond length (Å) ^a			Bond angle (°) ^a		
B3LYP/6-31G(d,p)		Exp ^b	B3LYP/6-31G(d,p)		Exp ^b
C1-C2	1.377	1.37618	C2-C1-C6	120.2	121.52109
C1-C6	1.420	1.41178	C2-C1-H17	120.9	119.26330
C1-H17	1.087	0.95134	C1-C2-C3	120.3	118.25816
C2-C3	1.418	1.41662	C1-C2-H11	120.1	122.54981
C2-H11	1.086	-	C6-C1-H17	119.0	119.21561
C3-C4	1.379	1.36013	C1-C6-C5	119.4	118.85850
C3-H12	1.086	0.94978	C1-C6-C7	123.6	123.74324
C4-C5	1.416	1.41786	C3-C2-H11	119.6	119.19061
C4-H18	1.085	0.94876	C2-C3-C4	120.9	122.35938
C5-C6	1.432	1.41763	C2-C3-H12	119.3	118.83488
C5-N10	1.367	1.36860	C4-C3-H12	119.8	118.80574
C6-C7	1.411	1.41614	C3-C4-C5	120.0	119.48196
C7-C8	1.383	1.37964	C3-C4-H18	122.0	120.25167
C7-H13	1.087	0.94877	C5-C4-H18	118.0	120.26637
C8-C9	1.429	1.42895	C4-C5-C6	119.3	119.47317
C8-C15	1.488	1.46620	C4-C5-N10	118.8	118.46870
C9-N10	1.298	1.29861	C6-C5-N10	122.0	122.04528
C15-O16	1.217	-	C5-N10-C9	118.4	117.72542
C15-H19	1.104	-	C6-C7-C8	120.9	121.06765

^a For numbering of atoms refer to Fig. 6.1

^b See Ref [12-29]

The calculated value of C=O bond length of the molecule is 1.217 Å which shows typical double bond characteristics. The DFT/B3LYP calculated C-C bond length for the compound is observed in the range 1.377-1.488 Å. This is in agreement with the reported values [15] of the bond lengths in similar quinoline complexes. The C-H bond length of the molecule is reported to be in the range 0.94867-0.95134 Å and the calculated value of C-H bond length for the compound is 1.085-1.104 Å. For the 8H5NC complex, the C-C-C and C-C-N bond angles are between 116.4-124.8⁰ and 118.8-125.3⁰ respectively. The reported values are of range 117.387-

123.743⁰ and 118.468-126.26⁰ respectively [13]. It is evident from the observed data that, all the bond angles are in good agreement with the observed values.

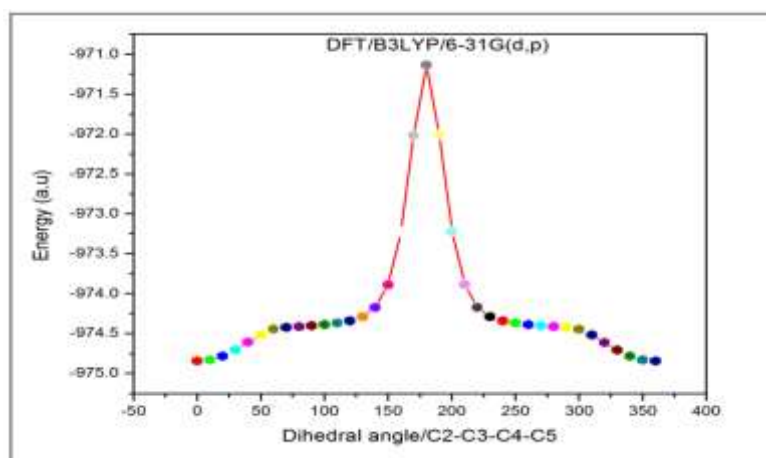


Fig. 2 Potential Energy Surface scan for dihedral angle C6-C1-N11-O20 of 8-hydroxy-5-nitroquinoline.

A potential energy scan with all the levels of theoretical approximation is performed along the C6–C1–N11–O20 torsional angle of 8H5NQ molecule in order to localize the structure that corresponds to the energy minima. All the geometrical parameters are simultaneously relaxed during the calculations, while the C2–C3–C4–C5 torsional angle is varied in steps of 10⁰. The resulting potential energy curve depicted in Fig. 2 shows that the minimum energy for this rotation is obtained at 0⁰ hence, the 0⁰ corresponds to the global minimum energy -974.839154 Hartrees.

Assignments of Vibrational spectra

The molecular structure 8H5NQ belongs to the C_s point group symmetry. The molecule consists of 20 atoms and is expected to have 54 normal modes, dispersed among the symmetry species as 37A' in-plane and 17A'' out-of-plane vibrations. Normal coordinate analysis is performed to provide a complete assignment of the fundamental vibrational wavenumbers of the molecule. The theoretically calculated DFT force fields are transformed to this latter set of vibrational coordinates and used in all subsequent calculations. The Potential energy distribution (PED) for each normal mode among the symmetry coordinates of the molecule is calculated. A complete assignment of the fundamentals is proposed based on the calculated PED values, FT-IR band intensities and FT-Raman activities. The unscaled B3LYP/6-31G(d,p) vibrational wavenumbers are generally larger than the experimental values. The reason for the disagreement between calculated and observed vibrational wavenumbers is that, the calculations are made for a free molecule in vacuum, while experiments are performed for solid sample. The reason is also partly due to the neglect of anharmonicity and partly due to approximate nature of the quantum mechanical methods. However, for reliable information on the vibrational properties the use of selective scaling is necessary. The calculated wavenumbers are scaled using the set of transferable scale factors recommended by Rauhut and Pulay [16].

The experimental and theoretical FT-IR and FT-Raman spectra are shown in Figs. 3 and 4 for comparative purposes, where the calculated intensity and activity are plotted against the harmonic vibrational frequencies. The experimental wavenumbers, calculated wavenumbers and IR intensities and Raman scattering activities are given in Table 4. In the table, we have given a detailed description of the normal modes based on the PED. All of the calculated modes are numbered from the biggest to the smallest frequency in the Table.

C-H group vibrations

In aromatic compounds, the C–H stretching wavenumbers appear in the range 3000–3100 cm⁻¹, and the C–H in-plane and out-of-plane bending vibrations appear in the range 1000–1300 cm⁻¹ and 750–1000 cm⁻¹ respectively [17,18]. Accordingly, in the present study, the five adjacent hydrogen atoms left around the rings of 8H5NQ give rise to five C–H stretching, five C–H in-plane bending and five C–H out-of-plane bending vibrations, which correspond to stretching modes of C4–H18, C2–H11, C7–H13, C3–H12, C1–H17, and C15–H19 units respectively. The aromatic C–H stretching of 8H5NCA give bands at 3059, 3042, 3013 and 2872

cm^{-1} in the FT-IR spectrum and at 3060, 3045, 2979 and 2875 cm^{-1} in the Raman spectrum. These modes are calculated from 3057 to 2855 cm^{-1} for 8H5NC. All the aromatic C–H stretching bands are found to be weak, and this is due to a decrease in the dipole moment caused by reduction of negative charge on the carbon atom. The in-plane aromatic C–H bending vibration occurs in the region of 1300 – 1000 cm^{-1} . The bands are sharp but have weak to medium intensity. The C–H in-plane bending vibration observed at 1313, 1206, 1164, 1137 and 1134 cm^{-1} by the B3LYP method shows excellent agreement with FT-IR bands at 1297, 1214, 1165, 1131 and 1002 cm^{-1} and at 1216, 1170 and 1147 cm^{-1} in the FT-Raman spectrum. The aromatic C–H out-of-plane bending vibrations occur at the region below 1000 cm^{-1} . In the present study, the bands at 937, 918, 901, 832 and 736 cm^{-1} are assigned to in the calculated spectrum indicating that they belong to the C-H out-of-plane vibrations. These vibrations are observed at 940, 912, 871, 807 and 749 cm^{-1} in the FT-IR spectrum and at 916, 811 and 754 cm^{-1} in FT-Raman spectrum. The calculated results are in good agreement with the observed data [19,20].

C-C vibrations

The ring carbon–carbon stretching vibrations occur in the region of 1625 – 1430 cm^{-1} . In general, the bands are of variable intensity and are observed at 1625 – 1590 , 1590 – 1575 , 1540 – 1470 , 1460 – 1430 and 1380 – 1280 cm^{-1} from the wavenumber ranges given by Varsanyi [21] for the five bands in the region. In the present work, the wavenumbers observed in the FT-IR spectrum at 1614, 1578, 1542, 1490, 1454, 1371, 1333, 1318, 1045 and 1002 cm^{-1} are assigned to C–C stretching vibrations. The same vibrations in the FT-Raman are at 1614, 1584, 1490, 1456, 1386, 1336, 1321, 1247 and 1020 cm^{-1} . The ring-breathing mode at 777 cm^{-1} in FT-IR and the same vibration in FT-Raman at 745 cm^{-1} as a medium band coincide with the B3LYP/6-31G(d,p) predicted value at 788 cm^{-1} for the most stable form. The in-plane deformations are at higher wavenumbers than those of out-of-plane vibrations. The bands at 969, 773, 524 and 424 cm^{-1} in both FT-IR and FT-Raman spectrum are assigned to the C–C–C deformation of the phenyl ring. The ring C–CHO stretching vibration occurs in the region 1230 – 1160 cm^{-1} [22]. Thus, the 1206 cm^{-1} band arises from the C–CHO stretching.

C - N vibrations

The C=N stretching skeletal bands [23-25] are observed in the range 1627 – 1566 cm^{-1} . For the title compound the bands observed at 1578 and 1583 cm^{-1} in the FT-IR and FT-Raman spectrum respectively, are assigned to the C=N mode. The C-N stretching mode is observed at 1371 and 1386 cm^{-1} respectively in FT-IR and FT-Raman spectra, which is in good agreement with calculated band at 1370 cm^{-1} . For conjugated azines [26] the C=N mode is reported at 1553 cm^{-1} . DFT calculations give these modes at 1566 and 1535 cm^{-1} .

C - O vibrations

Owing to the electronegativity differences between the carbonyl carbon and nitrogen atom of pyrazine ring, the C=O bond has a large dipole moment. The C=O stretching vibration band can be easily identified from the IR and Raman spectra, and because of the degree of conjugation, the strength and polarizations are increasing. In our case the C=O stretching band with strong intensity is observed at 1710 cm^{-1} in both FT-IR and FT-Raman spectra. Since the C=O group is a terminal group, only the carbon is involved in a second chemical bond. This reduces the number of force constants determining the spectral position of the vibrations.

Table 2: Detailed assignments of fundamental vibrations of 8-hydroxy-5-nitroquinoline by normal mode analysis based on SQM force field calculations using B3LYP/6-31G(d,p).

S. No	Symmetry	Experimental (cm^{-1})		Scaled freq. (cm^{-1})	Intensity		Characterization of normal modes with PED (%) ^d
		FT-IR	FT-Raman		I _{IR} ^b	I _{RA} ^c	
1	A ⁺	3059ms	3060s	3057	0.060	23.00	vCH(99)
2	A ⁺	3042s	3045ms	3045	0.111	27.30	vCH(99)
3	A ⁺	-	-	3037	0.050	18.70	vCH(99)
4	A ⁺	-	-	3031	0.059	18.00	vCH(99)
5	A ⁺	3013vw	2979vw	3023	0.021	8.93	vCH(99)
6	A ⁺	2872s	2875s	2855	0.387	14.00	vCHsub(99)
7	A ⁺	1687vs	1683vs	1685	0.856	34.40	vCO(70), β CHsub (17)
8	A ⁺	1614ms	1614s	1614	0.191	33.30	vCC(62), β CH(22)
9	A ⁺	1578s	1583s	1566	1.000	49.30	vCC(54), β CH(20), vCN(10)
10	A ⁺	1542vw	-	1547	0.426	31.60	vCC(57), β CH(13), vCN(12)
11	A ⁺	1490ms	1490ms	1497	0.166	13.70	β CH(46), vCC(40)
12	A ⁺	1454ms	1456vw	1461	0.162	5.70	β CH(50), vCC(31)
13	A ⁺	1418vw	1413w	1429	0.065	8.75	β CHsub (65), vCC(13)
14	A ⁺	1371ms	1386vs	1370	0.501	59.00	vCC(47), β CH(15), vCN(14)
15	A ⁺	1333ms	1336w	1348	0.191	100.0	vCC(74), vCN(12)

16	A ⁺	1318vw	1321w	1320	0.386	18.80	vCC(33), vCN(32), βCH(29)
17	A ⁺	1297vw	-	1313	0.178	20.20	βCH(30), vCC(29), vCN(15)
18	A ⁺	-	1247vw	1247	0.014	5.13	vCC(35), βCH(27), Rsym(18)
19	A ⁺	1214w	1216vw	1206	0.017	3.73	βCH(43), vCC(34), vCN(17)
20	A ⁺	1165s	1170w	1164	0.121	9.30	βCH(41), vCC(40), vCN(10)
21	A ⁺	-	1147ms	1137	0.184	11.80	vCC(44), βCH(24), vCN(17)
22	A ⁺	1131ms	-	1134	0.217	11.90	vCC(46), βCH(36)
23	A ⁺	1045vs	1020ms	1029	0.775	4.65	vCC(32), Rsym(22), Rtri(17)
24	A ⁺	1002vw	-	1005	0.048	19.90	vCC(76), βCH(17)
25	A ⁺	970w	970vw	977	0.013	8.36	ωCH(87)
26	A ⁺	940ms	-	937	0.011	0.49	τRtri(38), ωCH(37), τRasy(24)
27	A ⁺	912ms	916vw	918	0.068	1.38	ωCH(65), τRasy(22), τRtri(11)
28	A ⁺	-	-	907	0.111	2.90	Rtri(50), Rsym(13), vCC(12)
29	A ⁺	871w	-	901	0.067	2.73	ωCH(83), τRasy(8)
30	A ⁺	807s	811ms	832	0.016	4.61	τRasy(37), τRtri(32), ωCH(28)
31	A ⁺	777s	754s	788	0.126	23.20	vCC(36), βCO(14)
32	A ⁺	760s	-	736	0.258	37.60	vCC(38), τRasy(24), Bco(11)
33	A ⁺	749s	-	736	0.258	37.60	ωCH(47), τRtri(46)
34	A ⁺	678w	-	721	0.121	8.23	τRasy(50), τRtri(41)
35	A ⁺	621vw	-	638	0.012	0.82	τRtri(50), τRasy(46)
36	A ⁺	603	-	626	0.012	1.83	Rsym(37), Rtri(35), Rasy(14)
37	A ⁺	593w	-	593	0.039	4.41	vCC(23), βCO(22), Rsym(13)
38	A ⁺	-	-	585	0.078	5.53	Rasy(44), Rsym(18)
39	A ⁺	-	-	502	0.010	0.92	τRtri(53), τRasy(43)
40	A ⁺	485s	480vw	480	0.153	9.60	Rsym(20), vCC(16)
41	A ⁺	474ms	-	474	0.076	5.49	BUTTER (35), τRtri(31), τRasy(17)
42	A ⁺	420s	422vw	419	0.002	4.93	τRtri(33), τRasy(23), ωCC(22)
43	A ⁺	366w	368vs	361	0.024	34.40	vCC(28), Rtri(25), βCO(18)
44	A ⁺	344s	302vw	348	0.067	60.40	vCC (49), Rasy(32)
45	A ⁺	-	264vw	290	0.003	13.60	τRsym(24), ωCC(20), ωCH(19)
46	A ⁺	-	225w	244	0.003	3.06	τRasy(55), τRtri(28), τRsym(10)
47	A ⁺	-	190w	218	0.002	16.80	βCN (70), Rasy(12)
48	A ⁺	-	-	178	0.018	23.00	βCC(62), βCO(15)
49	A ⁺	-	137vs	134	0.071	18.90	τCO(53), τRtri(14), τRasy(10)
50	A ⁺	-	121s	100	0.007	94.90	BUTTER (22), τRtri(21), τCO(15)
51	A ⁺	-	-	75	0.005	4.61	τRasy(40), τRtri(29), τRsym(23)
52	A ⁺	-	-	67	0.121	23.20	Rtri(25), βCO(18), Rasy(16)
53	A ⁺	-	-	54	0.012	6.61	τRasy(24), Bco(11)

The carbon–oxygen double bond is formed by π – π bonding between carbon and oxygen. Because of the different electronegativities of the carbon and oxygen atoms, the bonding electrons are not equally distributed between the two atoms. The conjugation of C=O bond with C-O may increase its single bond character resulting in lowered values of carbonyl stretching wavenumbers. In our present study, we can expect one C-O stretching vibration observed at 1054 cm^{-1} in both FT-IR and FT-Raman spectra. The bond associated with the C=O stretching mode is found to be strongly and simultaneously active in both IR and Raman spectra.

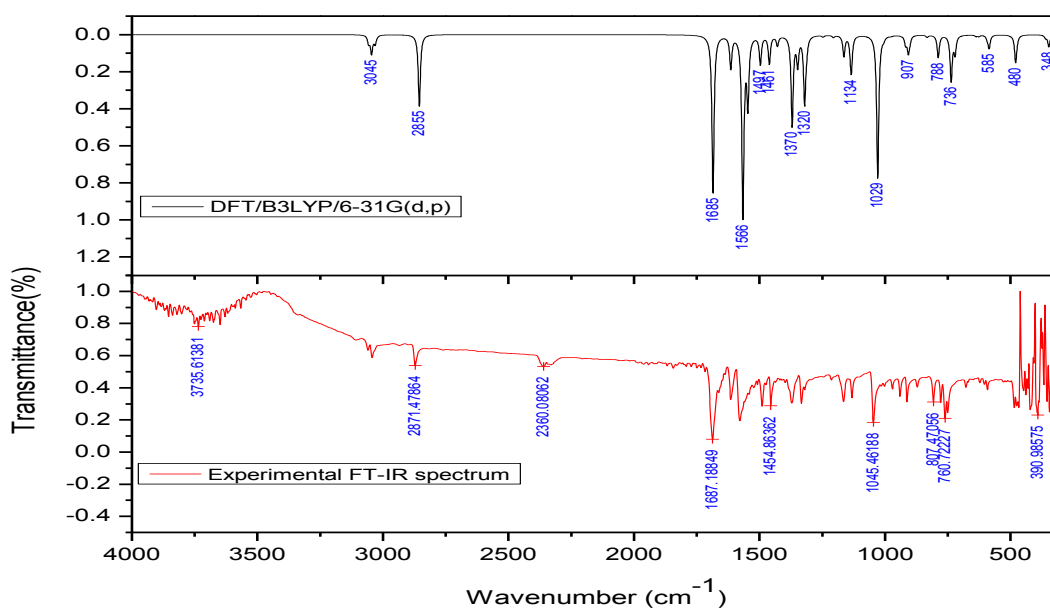


Fig.3 Experimental FT-IR and simulated FT-IR spectra of 8-hydroxy-5-nitroquinoline

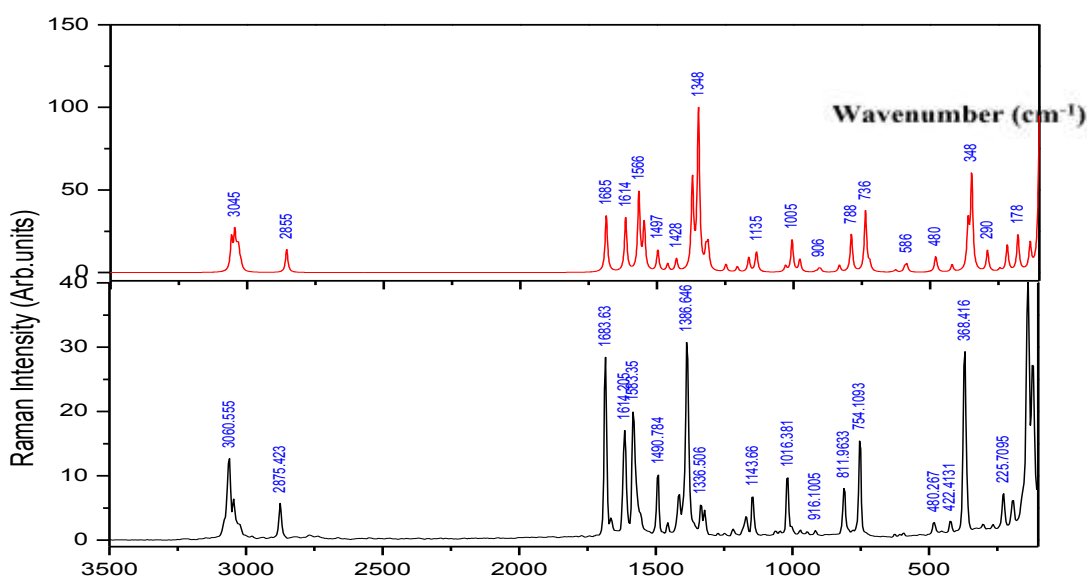


Fig 4 Experimental FT-Raman and simulated FT-Raman spectra of 8-hydroxy-5-nitroquinoline.

Nonlinear Optical (NLO) Properties

The dipolemoment (μ), second order-polarizability (α) and first hyperpolarizability (β_0) of this novel molecular system are calculated using HF/6-31G(d,p) basis set, based on the finite field approach. The calculated first hyperpolarizability of the title compound is 2.834×10^{-30} esu (Table 3), which is comparable with the reported values of similar quinazoline derivatives but experimental evaluation of this data is not readily available. The HF/6-31G(d,p) calculated total molecular dipole moment and average polarizability of 8H5NC are 1.3890 Debye and 38.8263×10^{-24} esu respectively shown in Table 5. The calculated first hyperpolarizability is about ~ 23 times greater than that of urea. The above results show that title compound is good material for NLO applications. We conclude that the title compound is an attractive material for future studies of nonlinear optical properties.

Table 3: The electric dipole moment μ , the average polarizability α_{tot} and the first hyperpolarizability β_{tot} of 2-Chloro-3-quinolinecarboxaldehyde by HF/6-31G(d,p) method.

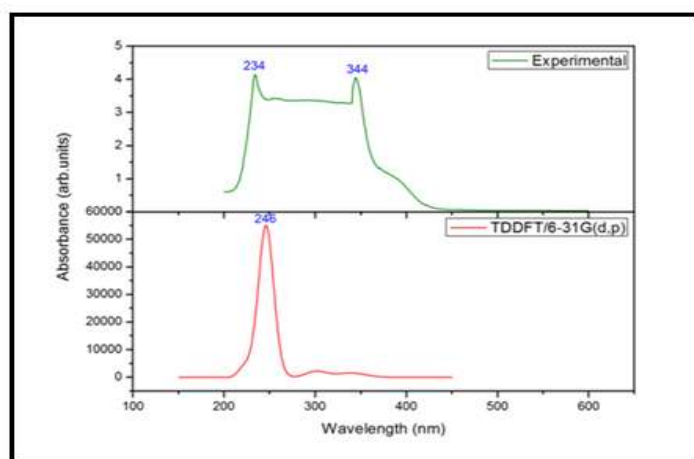
μ and α components	HF/6-31G(d,p)	β components	HF/6-31G(d,p)
μ_x	-0.797739	β_{xxx}	-81.996973
μ_y	0.001031	β_{xyy}	0.085069
μ_z	1.137193	β_{yyz}	3.924904
$\mu(D)$	1.389099	β_{yyy}	0.017823
α_{xx}	136.597549	β_{xxz}	87.144810
α_{xy}	-0.019529	β_{xyz}	0.002579
α_{yy}	41.517770	β_{yyz}	0.897547
α_{xz}	-26.580721	β_{xzz}	39.270573
α_{yz}	0.064690	β_{yzz}	-0.203092
α_{zz}	165.738219	β_{zzz}	-413.827263
$\langle\alpha\rangle(esu)$	38.8263×10^{-24}	$\beta_{total}(esu)$	2.8344×10^{-30}

Electronic absorption spectra and HOMO-LUMO analysis

On the basis of a fully optimized ground-state structure, the TD-DFT//B3LYP/6-31G(d,p) calculations have been used to determine the low-lying excited states of 8H5NQ is shown in Table 4. The calculated results involving the vertical excitation energies, oscillator strengths (f) and wavelengths are lifted along with measured experimental wavelengths. Typically, according to the Frank-Condon principle, the maximum absorption peak (λ_{max}) corresponds in a UV-visible spectrum to vertical excitation. The TD-DFT//B3LYP/6-31G(d,p) calculation predicts one intense electronic transition at 246.5 nm with an oscillator strength $f = 0.7183$, which is in good agreement with the measured experimental data ($\lambda_{exp} = 344$ nm) as shown in Fig 5. The UV-Vis spectrum is recorded for the compound in solid form which exhibit continuous absorption over a region. This is because the neighboring molecules interact with each other in solid form than it is in liquid form.

Table 4: The UV-vis excitation wavelength (λ), energy (E) and oscillator strength (f) calculated by TDDFT/B3LYP/6-31G(d,p) method for 8-hydroxy-5-nitroquinoline.

No.	Exp. λ (nm)	TDDFT/B3LYP/6-31G(d,p)			Symmetry	Major contributions
		E (cm ⁻¹)	λ (nm)	f		
1	344	29432	339.76	0.0213	Singlet-A	HOMO->LUMO (79%)
2	-	33202	301.17	0.0305	Singlet-A	HOMO-2->LUMO (51%),
3	257	39239	254.84	0.0003	Singlet-A	HOMO-3->LUMO+1 (89%)
4	-	40567	246.50	0.7183	Singlet-A	HOMO->LUMO+1 (44%)
5	234	42533	235.10	0.1295	Singlet-A	HOMO-2->LUMO+1 (70%)

**Fig. 5 Experimental (up) and calculated (down) using TDDFT UV-Visible spectra of 8-hydroxy-5-nitroquinoline.**

This electronic absorption corresponds to the transition from the ground to the first excited state and is mainly described by one electron excitation from the highest occupied molecular orbital (HOMO) to the lowest unoccupied molecular orbital (LUMO). The HOMO and LUMO energies and the energy gap for 8H5NQ calculated at the B3LYP/6-31G(d,p) level are shown in Table 5. The eigenvalues of LUMO and HOMO energy and their energy gap reflect the chemical activity of the molecule. The smaller the energy gap of LUMO and HOMO, the easier it is for the electrons of HOMO to be excited. The higher the energies of HOMO, the easier it is for HOMO to donate electrons; the lower the energies of LUMO, the easier it is for LUMO to accept electrons.

Table 5: The HOMO, LUMO energies and HOMO-LUMO energy gap for 8-hydroxy-5-nitroquinoline by using B3LYP/6-31G(d,p)

Property	8-hydroxy-5-nitroquinoline
Total energy (a.u)	-974.84969444
E_{HOMO} (eV)	-6.878820364
E_{LUMO} (eV)	-2.486323892
$\Delta E = E_{\text{HOMO}} - E_{\text{LUMO}}$ (eV)	4.392496472

Molecular Electrostatic Potential (MEP) surface

The MEP is related to the electronic density and is a very useful descriptor in determining the sites for electrophilic and nucleophilic reactions. The molecular electrostatic potential surface (MEP) which is a plot of electrostatic potential mapped onto the iso-electron density surface, simultaneously displays molecular shape, size and electrostatic potential values and has been plotted for both the molecules. To predict reactive sites for electrophilic and nucleophilic attack for the investigated molecule, the MEP at the B3LYP/6-31G(d,p) optimized geometry is calculated. The negative (red and yellow) regions of the MEP are related to electrophilic reactivity and the positive (blue) regions to nucleophilic reactivity, as shown in Fig 7. As can be seen from the Fig 6, this molecule has one possible site for electrophilic attack.

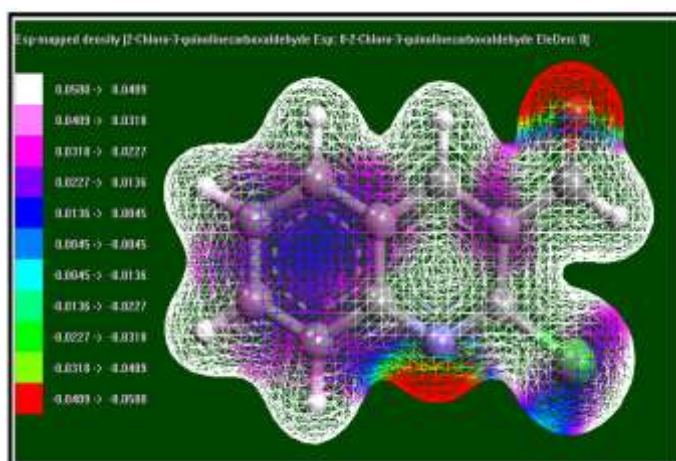


Fig .6 Molecular Electrostatic Potential energy surface (MEP) for 8-hydroxy-5-nitroquinoline.

According to these calculated results, the MEP map shows that the negative potential sites are on electronegative O and N atoms as well as the positive potential sites are around the hydrogen atoms. The predominance of green region in the MEP surfaces corresponds to a potential halfway between the two extremes, red and dark blue colours. These sites give information about the region from where the compound can have intermolecular interactions.

III. Conclusions

In present work, a detailed study of complete structural, vibrational and electronic properties of the title compound by using experimental techniques (FT-IR, FT-Raman and UV-Vis absorption spectra) and theoretical method (DFT/B3LYP/6-31G(d,p)). The scaled vibrational frequencies are in good agreement with the experimental data. The vibrational modes of the experimental wavenumbers are assigned on the basis of potential energy distribution (PED). The calculated first hyperpolarizability of 8H5NQ is about 23 times greater than that of urea. The above results show that the title compound is a good material for NLO applications. NBO analysis indicating the strong intramolecular hyperconjugative interaction within the molecule and stability of the molecule. In the UV-vis absorption spectrum one intense electronic transition $\pi \rightarrow \pi^*$ is observed at $\lambda_{\text{max}} = 344$ nm and the results of the DFT calculations gave the same as $\lambda_{\text{max}} = 246.5$ nm.

References

- [1] S. Levy, S. J. Azoulay, *Cardiovas. Electrophysiol.* 5 (1994) 635.
- [2] "Quinoline". *Encyclopædia Britannica*. 1911
- [3] O. Bilker, V. Lindo, M. Panico, A. E. Etienne, T. Paxton, A. Dell, M. Rogers, R. E. Sinden, H. R. Morris, *Nature*, 392 (1998) 289.
- [4] K. C. Fang, Y. L. Chen, J. Y. Sheu, T. C. Wang, C. C. Tzeng, *J. Med. Chem.* 43 (2000) 3809.
- [5] L. Y. Vargas, M. V. Castelli, V. V. Kouznetsov, J. M. Urbina, S. N. Lopez, M. Sortino, R. D. Enriz, J. C. Ribas, S. Zacchino, *Bioorg. Med. Chem.* 11 (2003) 1531.
- [6] L. Dassonneville, A. Lansiaux, A. Wattelet, N. Wattez, C. Mahieu, S. Van Miert, L. Pieters, C. Bailly, *Eur. J. Pharmacol.* 409 (2000) 9.
- [7] Z. Luo, C. Zeng, F. Wang, H. He, C. Wang, H. Du, L. Hu, *chem. res. chinese universities* 25 (2009) 841.
- [8] G. Jones, *Comprehensive Heterocyclic Chemistry II*; eds. A. R. Katritzky, C. W. Rees, E. F. Scriven, Eds, Pergamon: Oxford 5 (1996) 167.
- [9] C. J. Lee, R. B. Pode, D. G. Moon, and J. I. Han, *Thin Solid Films* 467 (2004) 201.
- [10] S. A. Jenekhe, X. Zhang, X. L. Chen, V. E. Choong, Y. Gao, B. R. Hsieh, *Chem. Letters.* 9 (1997) 409.
- [11] X. Zhang, A. S. Shetty, S. A. Jenekhe, *Acta Polym.* 49 (1998) 52.
- [12] Umar Farooq Rizvi, Hamid Latif Siddiqui, Saeed Ahmad, Matloob Ahmad, Masood Parvez *Acta Cryst. C* 64 (2008) 547.
- [13] A. Jan lokaj, B. Viktor Ketzmann, Vladim machacek Cand ale halama, *Acta Cryst. C* 55 (1999) 1101.
- [14] Antonio Henao martfneza, Alirio R. Palma, A Ladimirv. Kouznetsova, Gerardfaguirre-Hernandezb, Chicote Fernando-Ortegab and Manuel Soriano-Garcfa-*Acta Cryst. C* 55 (1999) 1181.
- [15] N Okabe, Y Marunishi, *Acta Cryst. C* 59 (2003) m228.
- [16] G. Rauhut, P. Pulay, *J. Phys. Chem.* 99 (1995) 3099.
- [17] K. Rastogi, M. A. Palafox, R. P. Tanwar, L. Mittal, *Spectrochim. Acta Part A* (2002) 1989.
- [18] M. Silverstein, G. Clayton Basseler, C. Morill, *Spectrometric Identification of Organic Compounds*, Wiley: New York, 1981.
- [19] G. Keresztury, *Raman spectroscopy: theory*, in: J.M. Chalmers, P.R. Griffiths (Eds.), *Handbook of Vibrational Spectroscopy*, vol. 1, John Wiley and Sons, 2002, p. 71.
- [20] Krishnakumar, N. Prabavathi, S. Muthunatesan, *Spectrochim. Acta Part A* 70 (2008) 991
- [21] G. Varsanyi, *Assignments for Vibrational Spectra of Seven Hundred Benzene Derivatives*, Vol. 1 and 2, Academic Kiado: Budapest, 1973.
- [22] G. Socrates, *Infrared and Raman Characteristic Group Frequency*, third ed., Wiley, New York, 2001.
- [23] Yalcin, E. Sener, O. Ozden, A. Aking, *Eur. J. Med. Chem.* 25 (1990) 705.
- [24] R. Saxena, L. D. Kaudpal, G.N. Mathur, *J. Polym. Sci., Part A: PolymChem.* 40 (2002) 3959.
- [25] R. M. Silverstein, F. X. Webster, *Spectrometric Identification of Organic Compounds* (6th edn), Wiley: Singapore, 2003.
- [26] M. Engasser, C. Horvath, *Biochem. J.* 45 (1975) 43158.